Journal of Southeast University (English Edition) Vol. 31, No. 1, pp. 46 - 50 Mar. 2015 ISSN 1003—7985

# Performance evaluation of wavelet scattering network in image texture classification in various color spaces

Wu Jiasong[1,4] Jiang Longyu[1,4] Han Xu[1,4] Lotfi Senhadji[2,3,4] Shu Huazhong[1,4]

([1]Key Laboratory of Computer Network and Information Integration of Ministry of Education, Southeast University, Nanjing 210096, China)

([2]Institut National de la Santé et de la Recherche Médicale U 1099, Rennes 35000, France)

([3]Laboratoire Traitement du Signal et de l'Image, Université de Rennes 1, Rennes 35000, France)

([4]Centre de Recherche en Information Biomédicale Sino-français, Southeast University, Nanjing 210096, China)

**Abstract:** The optimized color space is searched by using the wavelet scattering network in the KTH_TIPS_COL color image database for image texture classification. The effect of choosing the color space on the classification accuracy is investigated by converting red green blue (RGB) color space to various other color spaces. The results show that the classification performance generally changes to a large degree when performing color texture classification in various color spaces, and the opponent RGB-based wavelet scattering network outperforms other color spaces-based wavelet scattering networks. Considering that color spaces can be changed into each other, therefore, when dealing with the problem of color texture classification, converting other color spaces to the opponent RGB color space is recommended before performing the wavelet scattering network.

**Key words:** wavelet scattering network; color texture classification; color spaces; opponent mechanism

**doi:** 10.3969/j.issn.1003-7985.2015.01.008

Texture plays an important role in many image analysis techniques such as image segmentation, image retrieval, and image classification. Due to its importance, texture feature description has attracted much attention in the past decades. Lowe[1] proposed a famous data-dependent local feature descriptor, namely, scale-invariant feature transform (SIFT), which computes the local sum of image gradient amplitudes among image gradients having nearly the same direction in a histogram with eight different direction bins. Tola et al.[2] proposed a data-independent descriptor, known as DAISY, to approximate SIFT coefficients by $S[\lambda_1]x = |x * \psi_{\lambda_1}| * \varphi_{2^J}(u)$, where $\psi_{\lambda_1}$ are partial derivatives of a Gaussian computed at the finest image scale, along eight different rotations. The averaging filter $\varphi_{2^J}$ is a scaled Gaussian. Mallat et al.[3-4] proposed a new data-independent feature descriptor, that is, the wavelet scattering network (ScatNet). It can be seen as a multilayer version of DAISY, which substitutes the partial derivatives of a Gaussian by complex wavelets. Note that the above descriptors are mainly proposed for grey-scale images.

As we know, color provides useful information for image classification and object recognition[5-7]. For example, Van de Sande et al.[5] evaluated various color descriptors for object and scene recognition and concluded that the opponent SIFT is recommended when a single descriptor is chosen and no prior knowledge about the data set and object and scene categories is available. Zhang et al.[6] further extended the idea of the opponent SIFT to double opponent SIFT, which took red-cyan (R-C) channel into consideration. Oyallon et al.[7] extended the grey-scale ScatNet descriptor to color one; however, they only considered the YUV color space.

In this paper, we will consider wavelet scattering networks in various color spaces, and try to find the best color spaces for the utilization of wavelet scattering networks.

## 1 Color Spaces

Tab. 1 lists the color spaces considered in this paper. The conversions of some color spaces are shown as follows:

1) Converting RGB to YCbCr

$$\begin{bmatrix} Y \\ \mathrm{Cb} \\ \mathrm{Cr} \end{bmatrix} = \frac{1}{256}\begin{bmatrix} 65.481 & 128.553 & 24.966 \\ -37.797 & -74.203 & 112.0 \\ 112.0 & -93.786 & -18.214 \end{bmatrix}\begin{bmatrix} R \\ G \\ B \end{bmatrix} + \begin{bmatrix} 16 \\ 128 \\ 128 \end{bmatrix} \quad (1)$$

2) Converting RGB to $I_1I_2I_3$

$$\begin{bmatrix} I_1 \\ I_2 \\ I_3 \end{bmatrix} = \begin{bmatrix} 1/3 & 1/3 & 1/3 \\ 1/2 & 0 & -1/2 \\ -1/4 & 1/2 & -1/4 \end{bmatrix}\begin{bmatrix} R \\ G \\ B \end{bmatrix} \quad (2)$$

**Received** 2014-07-08.

**Biography:** Wu Jiasong (1983—), male, doctor, lecturer, jswu@seu.edu.cn.

**Foundation items:** The National Basic Research Program of China (No. 2011CB707904), the National Natural Science Foundation of China (No. 61201344, 61271312, 11301074), the Natural Science Foundation of Jiangsu Province (No. BK2012329), the Specialized Research Fund for the Doctoral Program of Higher Education (No. 20110092110023, 20120092120036).

**Citation:** Wu Jiasong, Jiang Longyu, Han Xu, et al. Performance evaluation of wavelet scattering network in image texture classification in various color spaces[J]. Journal of Southeast University (English Edition), 2015, 31(1): 46 - 50. [doi: 10.3969/j.issn.1003-7985.2015.01.008]

3) Converting RGB to CIE XYZ

$$\begin{bmatrix} X \\ Y \\ Z \end{bmatrix} = \frac{1}{0.177}\begin{bmatrix} 0.49 & 0.31 & 0.20 \\ 0.177 & 0.812 & 0.011 \\ 0.00 & 0.01 & 0.99 \end{bmatrix}\begin{bmatrix} R \\ G \\ B \end{bmatrix} \tag{3}$$

4) Converting RGB to HSL

$$r = \frac{R}{R+G+B}, \quad g = \frac{G}{R+G+B}, \quad b = \frac{B}{R+G+B}$$

$$\alpha = \max(r, g, b), \quad \beta = \min(r, g, b)$$

$$L = (\alpha + \beta)/2$$

$$S = \begin{cases} 0 & L = 0 \text{ or } \alpha = \beta \\ \dfrac{\alpha-\beta}{\alpha+\beta} = \dfrac{\alpha-\beta}{2L} & 0 < L \leqslant \dfrac{1}{2} \\ \dfrac{\alpha-\beta}{2-(\alpha+\beta)} = \dfrac{\alpha-\beta}{2-2L} & L > \dfrac{1}{2} \end{cases}$$

$$H = \begin{cases} 0^\circ & \alpha = \beta \\ 60^\circ \times \dfrac{g-b}{\alpha-\beta} + 0^\circ & \alpha = r \text{ and } g \geqslant b \\ 60^\circ \times \dfrac{g-b}{\alpha-\beta} + 360^\circ & \alpha = r \text{ and } g < b \\ 60^\circ \times \dfrac{b-r}{\alpha-\beta} + 120^\circ & \alpha = g \\ 60^\circ \times \dfrac{r-g}{\alpha-\beta} + 240^\circ & \alpha = b \end{cases} \tag{4}$$

5) Converting RGB to opponent RGB[5]

$$\begin{bmatrix} O_{11} \\ O_{12} \\ O_{13} \end{bmatrix} = \begin{bmatrix} 1/\sqrt{2} & -1/\sqrt{2} & 0 \\ 1/\sqrt{6} & 1/\sqrt{6} & -2/\sqrt{6} \\ 1/\sqrt{3} & 1/\sqrt{3} & 1/\sqrt{3} \end{bmatrix}\begin{bmatrix} R \\ G \\ B \end{bmatrix} \tag{5}$$

6) Converting RGB to double opponent RGB[6]

$$\begin{bmatrix} O_{21} \\ O_{22} \\ O_{23} \\ O_{24} \end{bmatrix} = \begin{bmatrix} 1/\sqrt{2} & -1/\sqrt{2} & 0 \\ 2/\sqrt{6} & -1/\sqrt{6} & -1/\sqrt{6} \\ 1/\sqrt{6} & 1/\sqrt{6} & -2/\sqrt{6} \\ 1/\sqrt{3} & 1/\sqrt{3} & 1/\sqrt{3} \end{bmatrix}\begin{bmatrix} R \\ G \\ B \end{bmatrix} \tag{6}$$

For more information about color spaces, we refer to Refs. [8 − 9].

## 2 Wavelet Scattering Network

The complex band-pass filter $\psi_\lambda$ is constructed by scaling a mother filter $\psi$ by $2^j$ and then rotating the filter $\psi$ by $\theta$, that is,

$$\psi_\lambda(x) = 2^{2j}\psi(2^j\theta^{-1}x) \qquad \lambda = 2^j\theta \tag{7}$$

with $0 \leqslant j \leqslant J-1$, and $\theta = k\pi/K$, $k = 0, 1, \ldots, K-1$.

The wavelet-modulus coefficients of $f(x)$ are given by

$$U[\lambda]f(x) = |f * \psi_\lambda(x)| \tag{8}$$

The scattering propagator $U[p]$ is defined by cascading wavelet-modulus operators[3],

$$U[p]f(x) = U[\lambda_m]\ldots U[\lambda_2]U[\lambda_1]f(x) = \big|\big|\big|f * \psi_{\lambda_1}| * \psi_{\lambda_2}| \ldots * \psi_{\lambda_m}(x)| \tag{9}$$

where $p = (\lambda_1, \lambda_2, \ldots, \lambda_m)$ are the frequency-decreasing paths, that is, $|\lambda_k| \geqslant |\lambda_{k+1}|$, $k = 1, 2, \ldots, m-1$.

Scattering operator $S_J$ performs a spatial averaging in a domain whose width is proportional to $2^J$.

$$S_J[p]f(x) = U[p]f * \varphi_J(x) = \big|\big|\big|f * \psi_{\lambda_1}| * \psi_{\lambda_2}| \ldots * \psi_{\lambda_m}(x)| * \varphi_J(x) \tag{10}$$

The wavelet scattering network is shown in Fig. 1.

The network nodes of the layer $m$ correspond to the set $P^m$ of all paths $p = (\lambda_1, \lambda_2, \ldots, \lambda_m)$ of length $m$. This $m$-th layer stores the propagated signals $\{U[p]f(x)\}_{p \in P^m}$ and outputs the scattering coefficients $\{S_J[p]f(x)\}_{p \in P^m}$. The output is obtained by cascading the scattering coefficients of every layer. We apply the wavelet scattering network to each channel of color images, and then cascade the scattering coefficients of each channel to form the final outputs.

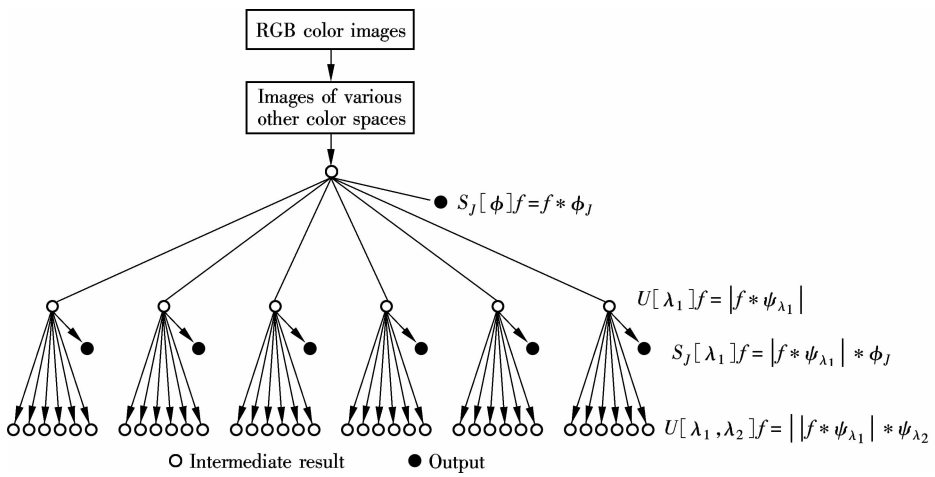


**Fig. 1** Three-layer wavelet scattering network

## 3 Numerical Experiment

In this section, the wavelet scattering network is performed in various color spaces in the KTH_TIPS_COL database[10], which contains in total 81 color images and is divided into 10 classes. Some examples are shown in Fig. 2.

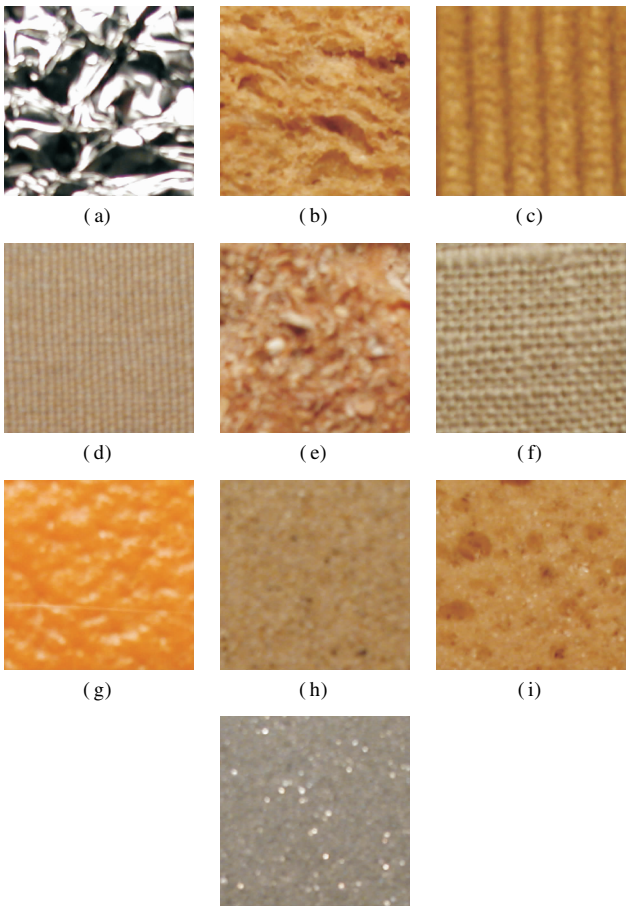

**Fig. 2** Some color image examples of KTH_TIPS_COL database(Color image size is $200 \times 200 \times 3$ pixels). (a) Aluminium foil; (b) Brown bread; (c) Corduroy; (d) Cotton; (e) Cracker; (f) Linen; (g) Orange peel; (h) Sandpaper; (i) Sponge; (j) Styrofoam

### 3.1 Preprocessing

We transfer all the color images in the KTH_TIPS_COL database from RGB space to various other color spaces as shown in Tab. 1.

### 3.2 Dividing

The total images of the KTH_TIPS_COL database are randomly divided into two parts, training data and testing data. In our experiment, 41 images are randomly chosen for training and the remaining 40 images for testing in each class. Therefore, we have 410 training images and 400 testing image in total.

### 3.3 Initialization

The parameters of the wavelet scattering network are initialized. We construct a three-layer scattering network by complex Gabor wavelets, whose finest scale is $2^J = 16$ and the total number of angles is $K = 8$. The oversampling factor is set to $2^1 = 2$. The corresponding scaling function covering the low frequency bands is a Gaussian function.

**Tab. 1** Various color spaces and their brief descriptions (six categories)

| Color spaces | Descriptions |
|---|---|
| RGB | Red, green, blue |
| YUV, YIQ, YPbPr, YCbCr, JPEG-YCbCr, YDbDr | Luminance, chrominance |
| HSV, HSL, HSI | Hue, saturation, value/lightness/intensity |
| $I_1I_2I_3$ | Linear transform of RGB |
| CIE XYZ, CIE LUV, CIE LCH, CIE LAB, CIE UVW, CAT02 LMS | Tristimuli, chromaticity, and colorimetric systems |
| Opponent RGB[8] Double opponent RGB[9] | Opponent theory |

### 3.4 Inputting training data to network

We put every image in the training set into the wavelet scattering network, which is shown in Fig. 1, and obtain the training characteristic matrix $\boldsymbol{Q}_0$, each column of which stores a scattering vector corresponding to one image.

The number of columns of the matrix corresponds to the number of training images. Each channel of color image is computed separately and their scattering coefficients are concatenated. For each channel of color image with size $200 \times 200$, a scattering vector of 417 dimensions is obtained. Therefore, for 410 training color images with three channels, we obtain a training characteristic matrix $\boldsymbol{Q}_0$ of size $1\ 251 \times 410$.

The image "brown bread" (see Fig. 2(b)) is taken as an example. Figs. 3(a) to (c) shows the first, second, and third layer scattering coefficients of the R-channel image of "brown bread", respectively. Note that we use the Matlab package "scatnet-0.2", which is available on the website[11].

### 3.5 Inputting testing data to the network

We put every image in the testing set into the wavelet scattering network (see Fig. 1), and obtain the testing characteristic matrix $\boldsymbol{Q}_1$. Similar to Section 3.4, for 400 testing images, the testing characteristic matrix $\boldsymbol{Q}_1$ of size $1\ 251 \times 400$ is obtained.

### 3.6 Concatenating

The matrices $\boldsymbol{Q}_0$ and $\boldsymbol{Q}_1$ are concatenated to obtain the scattering characteristic matrix $\boldsymbol{Q} = [\boldsymbol{Q}_0, \boldsymbol{Q}_1]$, whose size is $2\ 151 \times 810$, which represents the characteristics of the KTH_TIPS_COL database.

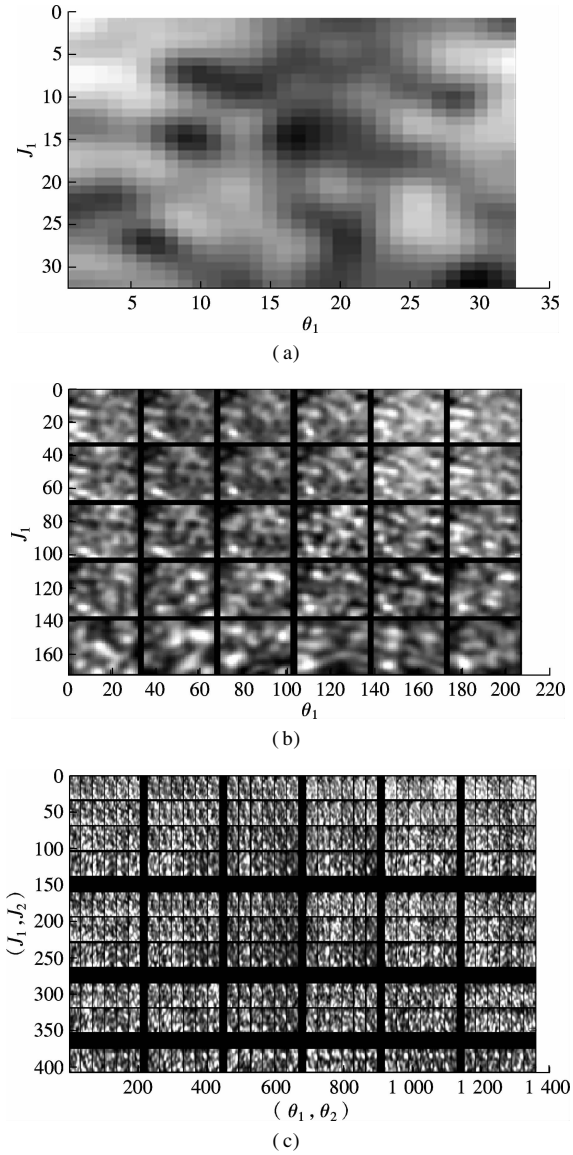


**Fig. 3** Scattering coefficients of R-channel of "brown bread". (a) First layer scattering coefficients; (b) Second layer scattering coefficients; (c) Third layer scattering coefficients

### 3.7 Classification

We put matrix $\boldsymbol{Q}$ into the linear principal component analysis (PCA) classifier, choose the dimensions of the principal component, and obtain the classification results, which are shown in Tab. 2. The classification results are averaged over 10 different random splits. From Tab. 2, we can see that the opponent-based color descriptors (opponent RGB and double opponent RGB) are superior to those of other color spaces, since opponent-based color descriptors are inspired by the opponent process theory[12] of human color vision. The intensity information is represented by channel $O_{13}$ and the color information by $O_{11}$ and $O_{12}$ in Eq. (5). Luminance-chrominance color spaces (YUV, YIQ, YPbPr, YCbCr, JPEG-YCbCr, YDbDr), CIE color systems (XYZ, LUV, LCH, LAB, CAT02 LMS) and $I_1I_2I_3$ achieve similar classification accuracies. Note that color spaces are separated into a luminance channel and chrominance channel, which are then separately processed, generally achieving a similar classification rate of color texture. Hue-saturation color spaces (HSV, HSL, HSI) achieve the worst classification accuracy. It seems that the color spaces with linear transforms of RGB are better than those of nonlinear transforms of RGB when dealing with color image texture classification.

## 4 Conclusion

In this paper, we give a comparison study of wavelet scattering networks in various color spaces for color texture classification in the KTH_TIPS_COL database. Opponent-based color descriptors are superior to those of other color spaces. Therefore, when a single descriptor is chosen and no prior knowledge about the data set is available, the opponent RGB wavelet scattering network is recommended and hue-saturation-based color spaces (HSV, HSL, HSI) are not recommended.

**Tab. 2** Classification accuracies of the wavelet scattering network in various color spaces in the KTH_TIPS_COL[10] database %

| Color spaces | Dimensions | | | | | | | | | |
|---|---|---|---|---|---|---|---|---|---|---|
| | 5 | 10 | 15 | 20 | 25 | 30 | 35 | 40 | 45 | 50 |
| RGB | 92.98 | 97.58 | 97.85 | 98.55 | 99.08 | 98.73 | 98.93 | 98.17 | 98.65 | 98.55 |
| YUV | 91.95 | 97.3 | 98.05 | 98.55 | 98.78 | 98.65 | 98.63 | 98.48 | 98.63 | 98.17 |
| YIQ | 93.05 | 97.65 | 97.65 | 98.53 | 98.38 | 98.55 | 98.68 | 98.33 | 98.68 | 98.38 |
| YPbPr | 92.87 | 97.45 | 97.88 | 98.30 | 98.68 | 98.43 | 98.40 | 98.75 | 98.55 | 98.53 |
| YCbCr | 92.48 | 97.47 | 98.08 | 98.48 | 98.60 | 98.50 | 98.53 | 98.73 | 98.53 | 98.88 |
| JPEG-YCbCr | 92.28 | 96.80 | 97.75 | 98.45 | 98.43 | 98.60 | 98.55 | 98.22 | 98.95 | 98.45 |
| YDbDr | 91.62 | 97.23 | 98.15 | 98.53 | 98.28 | 98.28 | 98.48 | 98.75 | 98.60 | 98.78 |
| HSV | 85.42 | 91.55 | 95.40 | 95.50 | 96.10 | 96.78 | 96.00 | 96.15 | 95.25 | 96.22 |
| HSL | 84.62 | 91.85 | 94.15 | 95.82 | 96.43 | 96.60 | 96.55 | 96.15 | 96.15 | 96.12 |
| HSI | 83.68 | 90.97 | 96.12 | 95.82 | 96.55 | 96.50 | 96.00 | 96.32 | 95.70 | 96.05 |
| $I_1I_2I_3$ | 92.98 | 97.25 | 97.98 | 98.45 | 98.30 | 98.75 | 98.48 | 98.28 | 98.43 | 98.13 |
| CIE XYZ | 93.83 | 97.60 | 98.00 | 98.25 | 98.15 | 98.55 | 98.73 | 98.68 | 98.65 | 98.65 |
| CIE LUV | 92.43 | 96.80 | 97.68 | 98.20 | 98.73 | 98.78 | 98.43 | 98.93 | 98.60 | 98.53 |
| CIE LCH | 92.70 | 97.05 | 97.70 | 98.45 | 98.53 | 98.23 | 98.43 | 98.93 | 98.70 | 98.75 |
| CIE LAB | 92.88 | 97.45 | 98.33 | 98.65 | 98.43 | 98.58 | 98.73 | 98.50 | 99.00 | 98.48 |
| CAT02 LMS | 93.50 | 97.20 | 97.82 | 98.53 | 98.83 | 98.78 | 98.88 | 98.35 | 98.48 | 98.80 |
| Opponent RGB | 94.55 | 98.93 | 98.95 | 99.28 | 99.53 | 99.33 | 99.38 | 99.00 | 99.43 | 99.38 |
| Double opponent RGB | 94.00 | 98.70 | 99.18 | 99.33 | 99.40 | 99.60 | 99.35 | 99.35 | 99.45 | 99.45 |

## References


[1] Lowe D G. Distinctive image features from scale-invariant keypoints [J]. *International Journal of Computer Vision*, 2004, **60**(2): 91 - 110.

[2] Tola E, Lepetit V, Fua P. DAISY: an efficient dense descriptor applied to wide-baseline stereo [J]. *IEEE Transactions on Pattern Analysis and Machine Intelligence*, 2010, **32**(5): 815 - 830.

[3] Mallat S. Group invariant scattering [J]. *Communications on Pure and Applied Mathematics*, 2012, **65**(10): 1331 - 1398.

[4] Bruna J, Mallat S. Invariant scattering convolution networks [J]. *IEEE Transactions on Pattern Analysis and Machine Intelligence*, 2013, **35**(8): 1872 - 1886.

[5] Van de Sande K E A, Gevers T, Snoek C G M. Evaluating color descriptors for object and scene recognition [J]. *IEEE Transactions on Pattern Analysis and Machine Intelligence*, 2010, **32**(9): 1582 - 1596.

[6] Zhang J, Barhomi Y, Serre T. A new biologically inspired color image descriptor [C]//*European Conference on Computer Vision*. Firenze, Italy, 2012: 312 - 324.

[7] Oyallon E, Mallat S, Sifre L. Generic deep networks with wavelet scattering [EB/OL]. (2014-03-10) [2014-06-22]. http://arxiv.org/abs/1312.5940.

[8] Ford A, Roberts A. Colour space conversions [EB/OL]. (1998-08-11) [2014-05-12]. http://www.poynton.com/PDFs/coloureq.pdf.

[9] Getreuer P. Colorspace transformations website [EB/OL]. (2010-09-21) [2014-04-20]. http://www.getreuer.info/home/colorspace.

[10] Fritz M, Hayman E, Caputo B. KTH-TIPS database [EB/OL]. (2006-06-09) [2014-05-22]. http://www.nada.kth.se/cvap/databases/kth-tips/.

[11] Mallat S. Scatnet Website [EB/OL]. (2010-09-01) [2014-05-22]. http://www.di.ens.fr/data/scattering/.

[12] Jain A, Healey G. A multiscale representation including opponent color features for texture recognition [J]. *IEEE Transactions on Image Processing*, 1998, **7**(1): 124 - 128.


# 小波散射网络在各种彩色空间进行图像纹理分类的性能比较


伍家松[1,4] 姜龙玉[1,4] 韩 旭[1,4] Lotfi Senhadji[2,3,4] 舒华忠[1,4]

([1] 东南大学计算机网络和信息集成教育部重点实验室, 南京 210096)

([2] 法国国家医学与健康研究院 U 1099, 法国 雷恩 35000)

([3] 雷恩第一大学信号与图像处理实验室, 法国 雷恩 35000)

([4] 东南大学中法生物医学信息研究中心, 南京 210096)



**摘要:** 为了寻找利用小波散射网络进行彩色图像处理的最佳彩色空间,用小波散射网络对 KTH_TIPS_COL 彩色图像数据库进行了图像纹理分类研究. 采用将彩色图像从 RGB 彩色空间转换到其他各种彩色空间的方法,研究了彩色空间的选择对于小波散射网络用于彩色图像纹理分类的影响. 实验结果表明:在不同的彩色空间对彩色图像纹理进行分类,分类成功率往往差别较大;在基于竞争机制的红绿蓝彩色空间中进行小波散射变换比其他彩色空间具有更好的分类性能. 考虑到彩色空间可以互相转换,对于彩色纹理图像的分类,推荐将彩色空间转化到基于竞争机制的红绿蓝彩色空间后再输入小波散射网络.



**关键词:** 小波散射网络; 彩色纹理分类; 彩色空间; 竞争机制

**中图分类号:** TP391